ISSN (Print) 1226-1750
ISSN (Online) 2233-6656
Journal of Magnetics 22(4), 637-641 (2017) https://doi.org/10.4283/JMAG.2017.22.4.637

Evaluation of the Specific Absorption Rate for Simultaneous Multi-Frequency RF Excitations in 7-T Magnetic Resonance Imaging

Jeung-Hoon Seo[1], Young Noh[2], Kyoung-Nam Kim[1]*, and Yeun Chul Ryu[1]*

[1]Neuroscience Research Institute, Gachon University, Incheon 21565, Republic of Korea
[2]Department of Neurology, Gachon University Gil Medical Center, Incheon 21565, Republic of Korea

(Received 19 September 2017, Received in final form 8 December 2017, Accepted 11 December 2017)

Radiofrequency (RF) safety in magnetic resonance imaging (MRI) is mainly verified using the specific absorption rate (SAR) in research involving humans. Universal MRI scanners measure the distribution of the hydrogen nucleus ^{1}H; hence, RF safety previously focused on the single frequency at which ^{1}H resonates. However, MRI technology is gradually transforming into simultaneous multi-frequency (MF) RF excitation to provide significant information related to biochemical changes in addition to morphological changes. These changes necessitate close monitoring of RF safety by considering other SAR aspects. This study proposes three evaluation methods for estimating the SAR value: summation of the SAR values of individual peaks, using the SAR value of the highest individual peak, and using the peak of the combined SAR for simultaneous RF excitation under MF RF excitation. This method, which is environmentally friendly, can be applied to various approaches for evaluating the RF safety in MF MRI applications.

Keywords : specific absorption rate (SAR), magnetic resonance imaging (MRI), radiofrequency (RF), multi-frequency (MF), 7-T (Tesla)

1. Introduction

In magnetic resonance imaging (MRI) of humans, the specific absorption rate (SAR) during radiofrequency (RF) energy deposition is a critical issue because of the resultant temperature increase in the affected biological tissue. The SAR values are mainly determined by the RF power absorbed per unit averaging volume. Thus, the SAR is determined by measuring the rate at which RF energy is absorbed by the human body when exposed to an RF electro-magnetic (EM) field, especially an electric (E)-field. The SAR limits are set by using various guidelines such as for the entire body, partial body, head, local, controlling mode 1st level controlling, 2nd level controlling, mass of 1 or 10-g, and the duration of exposure to RF.

Most MRI studies are based on the hydrogen nucleus (^{1}H) because ^{1}H nuclei give rise to a nuclear magnetic resonance (NMR) signal and are the most abundant nuclei in the human body [1]. Therefore, previously, MRI RF safety only focused on single-frequency RF excitation for ^{1}H. Other nuclei such as carbon (^{13}C), sodium (^{23}Na), and phosphorus (^{31}P) also have a net nuclear spin and can be imaged by using an MRI system. Measuring these nuclei reveals additional information about metabolite processes and disease-related biochemical changes, for example [2-8]. However, these nuclei are less abundant than ^{1}H in human tissue and require dedicated RF circuitry involving an optimal coil precisely tuned to their resonance frequency. Furthermore, a broadband spectrometer capable of measuring at several frequencies was necessary for specific MRI studies [9]. In standard multi-frequency (MF) RF excitation, known as multi-nuclear MRI, the signal of a second nucleus can be mostly obtained after acquiring the ^{1}H signal. Therefore, the total signal acquisition time can be multiplied by the number of nuclei. If simultaneous signal acquisition methods, namely MF RF excitation are employed, the total acquisition time could be reduced.

MF band RF excitation techniques have recently been commercially adopted in telecommunications to enhance the communication speed. The use of various antennas at the transmitter/receiver (Tx/Rx) exploits the multipath environment of a communication link and allows the

©The Korean Magnetics Society. All rights reserved.
*Co-Corresponding author: Tel: +82-32-820-4410
Fax: +82-32-460-8230, e-mail: yeunchul.ryu@gachon.ac.kr
Tel: +82-32-820-4263, Fax: +82-32-460-9015
e-mail: kyoungnam.kim@gachon.ac.kr

© 2017 Journal of Magnetics

system to have many independent channels. A multi-input and multi-output (MIMO) antenna comprises numerous antenna components that operate at MFs as both Tx and Rx. This approach prompted specific research that sought to establish a safety standard based on the SAR evaluation of the MIMO antenna [10, 11]. The value of SAR in MF RF energy was estimated by using different adaptations and definitions of methods to determine the limits of the energy that can be absorbed by the Tx.

In this study, we suggest and evaluate three different evaluation methods based on the aforementioned approach in the telecommunication field to estimate the value of SAR in MF RF excitations for human MRI applications [12]. All computational calculations were performed by using an electromagnetic (EM) field; more specifically, electric (E)-field simulations with a digital human model that satisfies safety regulations were used.

2. Experimental Methods

2.1. SAR specifications and standards

The SAR is the amount of RF energy from the coil absorbed by biological tissue and is defined as

$$SAR = \sigma \cdot E^2/2 \cdot \rho \quad (1)$$

where σ (S/m) and E (V/m) are the conductivity of human tissue and the E-field induced inside the human body. The other specific value of ρ (kg/m^3) is the density of the sample. Various standards specify different upper limits for the SAR to limit the potential health risks due to exposure to EM radiation. In telecommunications regulations, the maximum power deposition allowed by the Federal Communications Commission (FCC), expressed in SAR, is 1.6 W/kg for 1 g of tissue for exposure to cellular phone radiation (US and Canada) [13]. In contrast, international communication on non-ionizing radiation protection guidelines stipulate a maximum SAR of 2 W/kg for any 10 g of tissue in the head (EU, Japan, and Brazil) [14]. SAR limits for MRI safety regulations are different for applications wherein exposure to Tx power primarily occurs. The maximum power deposition allowed by the International Electrotechnical Commission (IEC), expressed in SAR, is provided in Table 1 [12].

2.2. Alternative MF SAR calculation

The evaluation of MF SAR requires the EM to be calculated for MF situations and a procedure to determine the SAR from each analysis. The procedure is based on the method used for MIMO SAR analysis in telecommunication systems. The following three methods for two different frequencies *i* and *ii* are defined as

Method I: summation of individual peak SAR values (*p*SAR_I)

$$pSAR_I = peak_SAR_i + peak_SAR_{ii} \quad (2)$$

Method II: select highest individual peak SAR values (*p*SAR_II)

$$pSAR_II = \max \{peak_SAR_i , peak_SAR_{ii}\} \quad (3)$$

Method_III: peak of combined SAR values (*p*SAR_III)

$$pSAR_III = peak \{peak_SAR_i + peak_SAR_{ii}\} \quad (4)$$

In the above equations, "*peak*" denotes a search for the peak maximum and "*max*{ }" indicates selecting the maximum value within the braces. The peak SAR can be obtained with methods I to III. In the case of simultaneous MF RF excitation in the MRI, the average SAR over multiple frequencies would need to be calculated instead of using a single peak to obtain the SAR value. Method III was utilized for calculating the average SAR value. That is, after obtaining the SAR at different frequencies, the two SAR values were added, and the average SAR corresponding to 1 g or 10 g was obtained by using the phantom mass information. In particular, the EM properties of human tissue such as the conductivity and permittivity were changed according to the frequency of the RF waves to which the tissue is exposed.

2.3. Two-frequency RF field simulation with a human object

The computational calculation of the EM field and SAR was conducted with the finite-different time-domain (FDTD) software, Sim4Life (Speag, Switzerland) [15]. The 8-channel dual-tuned (i.e., dual-frequency) simultaneous Tx/Rx loop coil was modeled as shown in Fig. 1. The

Table 1. IEC 60601-2-33(2010) patient and volunteer SAR limits (W/kg) for MRI RF field exposure. The value shows averaged SAR

	Whole body	Partial body			Local trunk	Extremities
		Head	Not head	Head		
Normal Mode	2	3.2	2-10	10	10	20
Controlled Mode	4	3.2	4-10	20	20	40
Research Mode	> 4	> 3.2	> (4-10)	> 20	> 20	> 40

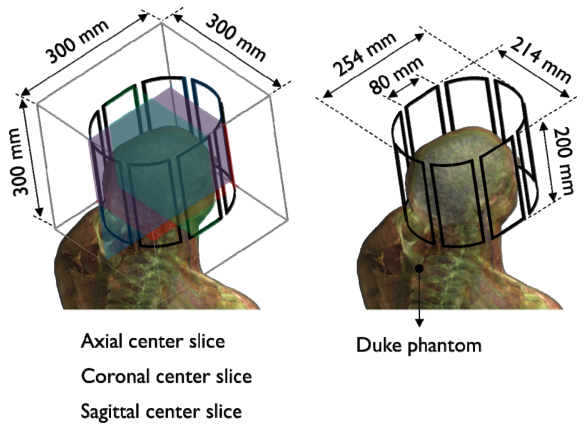

Fig. 1. (Color online) Simulation setup for electromagnetic field and SAR evaluation at different resonant frequencies of 120 MHz and 298 MHz. The 8-channel dual-frequency RF coil is combined with a human model (Duke) and designed to fit the head structure.

material of the coil is a perfect electric conductor (PEC) with a width and thickness of 5 mm and 1 mm, respectively. Each coil element has a rectangular shape and measures 80 mm × 200 mm. At the front and back, all the elements are curved to fit around the head. The operating frequency of the coil was set to different frequencies of 120 MHz and 298 MHz, for instance, which correspond to the frequencies of ^{31}P and ^{1}H in MRI, respectively, at 7-T. The high-resolution human model Duke (human model software from IT'IS Foundation [Information Technologies in Society], Switzerland) was used for EM field calculation and SAR evaluation [16]. The total grid size of the simulation is 329 × 354 × 293 cells for the x-, y-, and z-axes, respectively. The total number of cells is 34,125 M. The total input RF power is 288 V (4.5 V × 64 ports) with a geometrical phase for 298 MHz (^{1}H frequency at 7-T) and 452 V (7.0625 V × 64 port) with a geometrical phase for 120 MHz (^{31}P frequency at 7-T). The frequency-dependent tissue properties of conductivity and permittivity are assigned automatically by the Sim4Life simulator.

3. Results

3.1. Electromagnetic field analysis at a single frequency

The RF excitation (B_1^+) field and E-field of the model

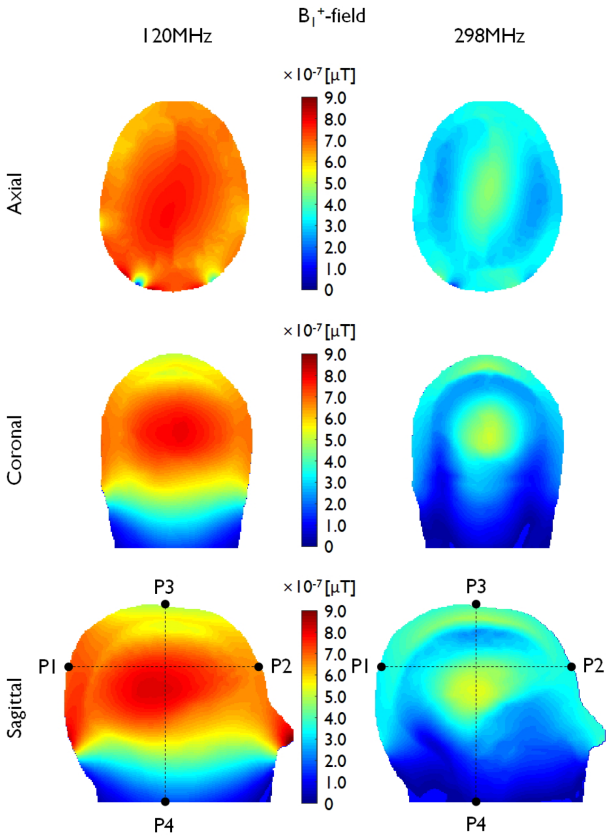

Fig. 2. (Color online) Magnetic-field simulation results for the frequencies 298 MHz and 120 MHz in the axial, coronal, and sagittal views.

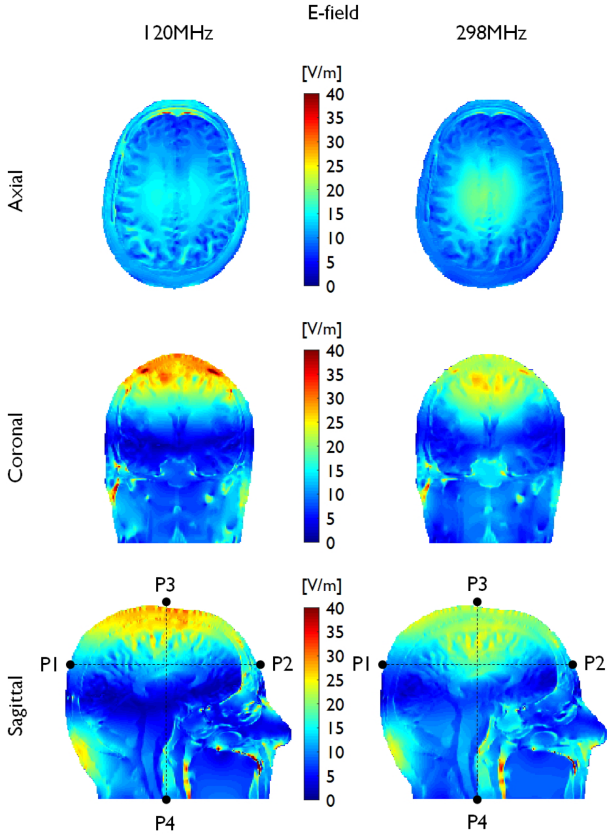

Fig. 3. (Color online) Electric-field simulation results for the frequencies 298 MHz and 120 MHz in the axial, coronal, and sagittal views.

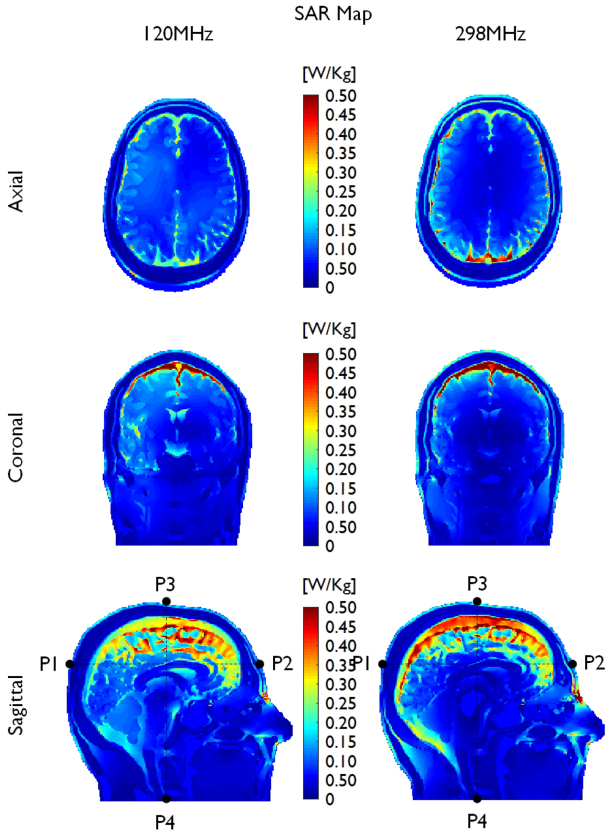

Fig. 4. (Color online) Maps of SAR for single-frequency RF excitation.

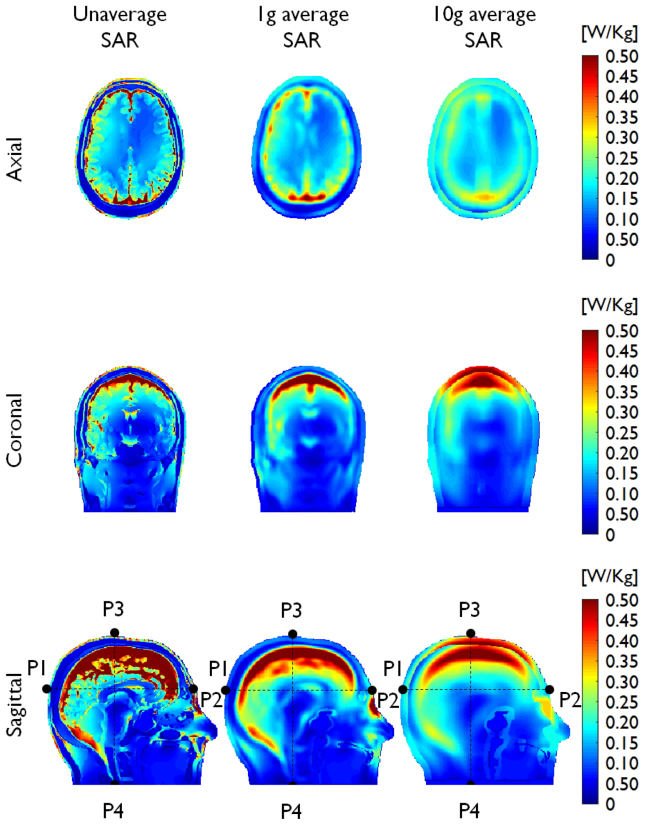

Fig. 5. (Color online) Maps of local and averaged SAR for simultaneous MF RF excitation with Method III in axial and sagittal view.

are shown in Fig. 2 and 3. The B_1^+ field pattern at 120 MHz is more homogeneous than at 298 MHz. The wavelength of RF excitation at 298 MHz was about 2.5 times shorter than at 120 MHz, which the EM field creates heterogeneously distributed in the overall area of the subject. The SAR map for each excitation is as shown in Fig. 4. The position of the peak SAR value and their SAR patterns exhibit different distributions. For RF excitation at 298 MHz, the peak SAR was distributed in the cortex area; however, for RF excitation at 120 MHz, the SAR is high in the mid-brain area. The SAR pattern is also different from the E-field pattern, as the mass of the tissue is included in the SAR calculation.

3.2. Combined SAR of two-frequency excitation

The combined SAR values using Method III are shown in Fig. 5. The unaveraged SAR obtained from the pixel-wise summation of two local SARs is shown in the column on the left. The center column shows the average SAR for 1 g, whereas the column on the right shows the average SAR for 10 g. The unit of the indexed color is set to W/kg. When Method III is used, the peak SAR values are located at the top of the brain cortex area on these maps of the average SAR for 1 g or 10 g.

Table 2 lists the peak SARs from the single-frequency RF excitation and Methods I to III. Method I, i.e., the addition of two peak values from each frequency excita-

Table 2. Peak SARs for single and simultaneous excitation. Mass-averaged SARs (1 g SAR, 10 g SAR) are calculated from the tissue information of the human model.

[W/Kg]	298 MHz	120 MHz	Method I	Method II	Method III
Peak Unaveraged SAR	1.2659	2.0355	3.3014	2.0355	3.3014
Peak Local SAR	1.2659	2.0355	3.3014	2.0355	3.3014
Peak 1 g SAR	0.4260	0.5443	0.9606	0.5443	0.9606
Peak 10 g SAR	0.2869	0.3345	0.6181	0.3345	0.6181

tion, does not require additional simulation other than a single SAR calculation. However, the results also show much higher SAR values, as in Method III. Method II produces lower values because this method compares two peak SARs and selects the higher value.

3.3. Discussion and Conclusion

In this study, we evaluated the calculation of SAR for the dual-frequency Tx/Rx RF coil in MRI. This takes into account that a volume coil and Tx/Rx loop coil would have a different SAR values and distributions. Continued research may help to establish a reference safety standard for simultaneous MF RF excitation in terms of SAR, which is extended to multi-nuclear MR experiments. These results may also be applied to various MF experiments, even those not involving simultaneous RF excitation. For instance, our simulation results are also applicable to the sequential RF excitation of different nuclei in single repletion time (TR) experiments. RF shimming of the magnetic flux density (B_1) could be used to reduce the SAR by optimizing the E- and B_1-field over the subject. Although we did not consider B_1 shimming or other B_1 field-optimizing methods, in experiments requiring extremely high RF power, B_1 shimming would be required to overcome the high degree of RF energy absorption. If the limitation of SAR is critical for an experiment involving a normal simultaneous multi-nuclear excitation method, simultaneous hyperpolarized spin methods would be a viable alternative although the details are beyond the scope of this study.

Simultaneous MF RF excitation of more than three frequencies would be acceptable in ultra-high-field MRI applications because of the intrinsically high signal-to-noise ratio and spectrum separability. We are currently studying the simultaneous excitation of three different RF frequencies, for instance, ^{23}Na, ^{31}P, and ^{1}H. The temperature increase in the subject following RF exposure is another safety criterion of medical imaging systems, and performing temperature experiments with simultaneous MF excitation is our next research target.

Acknowledgments

This research was supported by a grant from the Korea Health Technology R&D Project through the Korea Health Industry Development Institute, funded by the Ministry of Health & Welfare, Republic of Korea (grant number: HI14C1135). This work was supported by the Gachon University Gil Medical Center. (Grant number: 2015-19). We would like to thank ZMT for providing a free license for the Sim4Life software used in this study.

References

[1] C. H. Choi, S. M. Hong, Y. H. Ha, and N. J. Shah, Magn. Reson. **279**, 11 (2017).
[2] W. Negendank, NMR Biomed. **5**, 303 (1992).
[3] G. B. Matson, P. Vermathen, and T. C. Hill, Magn. Reson. Med. **42**, 173 (1999).
[4] R. F. Lee, R. Giaquinto, C. Constantinides, S. Souza, R. G. Weiss, and P. A. Bottomley, Magn. Reson. Med. **43**, 269 (2000).
[5] C. Mirkes, G. Shajan, G. Chadzynski, K. Buckenmaier, B. Bender, and K. Scheffler, Magn. Reson. Mater. Phys. **29**, 579 (2016).
[6] R. Brown, K. Lakshmanan, G. Madelin, L. Alon, G. Chang, D. K. Sodickson, R. R. Regatte, and G. C. Wiggins, Magn. Reson. Med. **76**, 1325 (2016).
[7] P. A. Bottomley, NMR Biomed. **29**, 187 (2016).
[8] C. Ma, Magn. Reson. Med. **78**, 419 (2017).
[9] Y. He, Z. Zhang, J. Feng, C. Huang, F. Chen, M. Liu, and C. Liu, Sci. China Chem. **59**, 830 (2016).
[10] G. P. Kumar, N. Agarwal, P. Kranthi, and S. S. Bau, IEEE WiSPNET Conference, 2434 (2016).
[11] P. Pinho, A. Lopes, J. Leite, and J. Casaleiro, in Proceedings of the International Conference on Electromagnetics in Advanced Applications (ICEAA' 09), 431 (2009).
[12] International Electrotechnical Commission, Particular requirements for the basic safety and essential performance of magnetic resonance equipment for medical diagnosis, **IEC 60601-2-33**, (2010).
[13] Health Canada, Limits of Human Exposure to Radiofrequency Electromagnetic Fields in the Frequency Range from 3 kHz to 300 GHz, **Safety Code 6** (2013).
[14] J. C. Lin, IEEE Antennas Propag. Mag. **42**, 138 (2001).
[15] Sim4Life by ZMT, www.zurichmedtech.com.
[16] Information Technologies in Society, http://www.itis.ethz.ch.